Asian Journal of Chemistry; Vol. 30, No. 8 (2018), 1723-1730

ASIAN JOURNAL OF CHEMISTRY

https://doi.org/10.14233/ajchem.2018.21275

Highly Porous MOF Adsorbent for Wastewater Treatment

NTAOTE DAVID SHOOTO* and EZEKIEL DIXON DIKIO

Applied Chemistry and Nano-Science Laboratory, Department of Chemistry, Vaal University of Technology P.O. Box X021, Vanderbijlpark 1900, South Africa

*Corresponding author: E-mail: davidshooto12@gmail.com

Received: 7 February 2018; *Accepted*: 15 March 2018; *Published online*: 30 June 2018; AJC-18963

Heavy metal detoxification is one of the major challenges in our generation. Metals such as Cu(II), Pb(II) and Ni(II) have a toxic effect to human health. Therefore, it is necessary to eliminate such metal ions from aqueous solutions. In this study, we report a newly developed cadmium metal organic framework (MOF) adsorbent for Cu(II), Pb(II) and Ni(II); namely cadmium benzene 1,2,4,5-tetracarboxylate (Cd-H_4bta MOF). This material was synthesized by refluxing; benzene 1,2,4,5-tetracarboxylic acid (H_4bta) was reacted with cadmium salt in dimethylformamide medium. The produced material was characterized by scanning electron microscopy, nitrogen adsorption-desorption analysis, thermogravimetric analyzer, X-ray diffraction and Fourier transformed infrared spectroscopy. Scanning electron microscopy images revealed that the highly porous rhombic prism crystals of variable sizes were synthesized and its morphology is reported for cadmium coordination compounds. TGA-DTA profiles showed the thermal behaviour of this material to be highly stable. Our proposed adsorbent material *i.e.*, Cd-H_4bta MOF consist of cadmium ions. Before use Cd-H_4bta MOF stability test in aqueous solution was conducted and it was found the material is insoluble and does not leach cadmium ions, therefore it is suitable and safe for aqueous solution use. Its adsorption capabilities to remove Cu(II), Pb(II) and Ni(II) ions from aqueous solutions were investigated using batch experiments by varying parameters such as initial concentration of metal ions and contact time; thereafter isotherms and kinetics were determined. The metal ions measurements before and after adsorption were carried out through atomic absorption spectroscopy. The Cd-H_4bta MOF adsorption capacities for Cu(II), Pb(II) and Ni(II); were 183.43, 171.42 and 120.31 mg/g respectively. Kinetics data of all targeted metals, followed pseudo second order model. The results indicated that Cd-H_4bta MOF is a promising adsorbent for Cu(II), Pb(II) and Ni(II) ions in aqueous media

Keywords: MOFs, Adsorption, Cadmium, Lead, Nickel, Copper.

INTRODUCTION

Heavy metals are widely used in many industries such as electroplating, mining, agriculture, oil companies and others. These industries led to high content of heavy metals being discharged to water [1-4]. Once these toxic metals are released in the environment they are introduced into the human body through breathing, consumption and skin absorption [5]. Exposure to heavy metals poses a serious risk to the environment and public health, due to their toxicity, mutagenesis and carcinogenic, overtime they accumulate in living tissues, inducing diseases and disorders in living human beings [6,7]. Lead(II) is a slow insidious but malignant poison, its chronic effects are colic, constipation and anaemia [8]. Copper(II) usually graft itself in the brain, liver, pancreas and myocardium [9]. Nickel(II) have ability to be stored in vital organs of the body and cause adverse side effects [10]. Removal of these heavy metal ions from wastewater is necessary before disposal to assure environmental and public health safety.

Various techniques such as adsorption, solvent extraction, chemical oxidation, ion-exchange and membrane filtration are employed methods for removing heavy metal from wastewater [11-15]. However adsorption is a superior and promising technology, due to its attributes of high removal efficiency, ease to conduct, low-cost, eco-friendly and does not require high operational temperatures [16]. Highly esteemed adsorbent for the removal of heavy metal ions from aqueous solution is commercial activated carbon. However, it suffers from disadvantage of moderate adsorption capacity. This drawback makes it unsuitable for practical applications, in the field of industrial effluents management [17,18].

Metal organic frameworks (MOFs) materials have been increasingly attracting attention in diverse areas of research due to their versatility, outstanding properties and performance [19,20]. Various studies have reported MOFs as potential candidates in catalysis, gas adsorption and separations, sensors and heavy metal removal from aqueous solution [21-25]. This is because of the structural properties provided by the MOFs;

highly porous and large surface area, high thermal and mechanical stability [26]. MOFs have developed beyond the point of being just another synthetic chemistry material; they have emerged as extensively applied materials.

Numerous cadmium based MOF materials have been reported. However fewer studies have exploited its capability to remove heavy metals from aqueous solution [27]. Therefore this research work is aimed at the synthesis of Cd-H_4bta MOF, its characterization and adsorption application towards the metal ions of Cu(II), Ni(II) and Pb(II). The effect of parameters such as concentration and contact time also studied. The reported material exhibited higher surface area and adsorptive capabilities.

EXPERIMENTAL

Cadmium acetate dihydrate [$Cd(CH_3COO)_2{\cdot}2H_2O$, > 98 %, Sigma-Aldrich], *N,N*-dimethylformamide [$HCON(CH_3)_2$, DMF, 99.8 %; AnalaR], benzene 1,2,4,5-tetracarboxylic acid [$C_6H_2(CO_2H)_4$,H_4bta, 96 %, Sigma-Aldrich], methanol [CH_3OH, 99.9 %, Sigma-Aldrich]. All the reagents were obtained from commercial sources and were used without further purification.

Synthesis of Cd-H_4bta MOF: Cd-H_4bta was produced by a reflux method. A solution was prepared by dissolving benzene 1,2,4,5-tetracarboxylic acid (3.05 g, 0.01 mol) and cadmium acetate (3.05 g, 0.01 mol) in 80 mL of N,N-dimethylformamide. The solution mixture was stirred and refluxed at 120 °C overnight. The resulting white crystalline material was isolated by centrifugation and washed with methanol several times to remove DMF. The obtained crystals were then dried in oven at 40 °C for 0.5 h and used for further experiments.

Preparation of standard solutions: Cu(II), Ni(II) and Pb(II) stock solutions of 100 mg/L were prepared by dissolving nitrate salt of each metal in ultrapure water respectively. The standard and working solutions were prepared by matrix dilutions of the stock solutions.

Adsorption experiments: Batch experiments were conducted by treating known concentration solutions of Cu(II), Ni(II) and Pb(II) ions with a weighed Cd-H_4bta. To investigate the concentration effect, 0.1 g of Cd-H_4bta was allowed to interact with 20 mL of Cu(II), Ni(II) and Pb(II) solutions respectively at different concentrations (20, 40, 60, 80 and 100 mg/L) each concentration was done in triplicate. The solutions were agitated on a shaker for 0.5 h. After the prespecified time, Cd-H_4bta was separated from the solutions by centrifugation. Time dependent studies, 0.1 g Cd-H_4bta was dispersed in 20 mL solutions of Cu(II), Ni(II) and Pb(II), 100 mg/L respectively at various time intervals (5, 10, 15, 20, 30, 40 and 60 min) each time interval was triplicated. After the specified time elapsed, the adsorbent was separated from the solutions by centrifugation. The supernatant solutions were stored for metal analysis.

Adsorption capacity (q_e, in mg/g) was calculated using eqn. 1:

$$q_e = \frac{V}{m}(C_o - C_e) \quad (1)$$

where, C_o is the initial concentration of the Cu(II), Ni(II) and Pb(II) in the solution (mg/L), C_e is the equilibrium concentration of the metal ions in the solution (mg/L), V is the volume of the solution (L) and m, is the mass of Cd-H_4bta used (g).

Removal percentage (R_p, in %) was determined from eqn. 2:

$$R_p = \frac{(C_o - C_e)}{C_o} \times 100 \quad (2)$$

Kinetic studies: Pseudo first order kinetic eqn. 3 was used to determine the followed adsorption model

$$\frac{dq_t}{dt} = k_1(q_e + q_t) \quad (3)$$

where k_1 is the rate constant for the first order adsorption (gm g^{-1} min^{-1}).

The pseudo second order kinetic model was determined using the following eqn. 4 [28].

$$\frac{t}{q_t} = \frac{1}{k_2 q_e^2} + \frac{1}{q_e}t \quad (4)$$

where k_2 is the pseudo second order kinetic rate constant of adsorption (gmg^{-1} min^{-1}) and q_t is metal ion adsorption capacity at time t.

Isotherm studies: Linearized Langmuir isotherm applicability was studied for Pb(II), Cu(II) and Ni(II) adsorption using the following linear expression. Where Q_e (mg/g) is the maximum adsorption capacity and K_L (dm^3/g) is Langmuir constant related to (R_L) rate of adsorption:

$$\frac{C_e}{q_e} = \frac{1}{Q_e K_L} + \frac{1}{Q_e}C_e \quad (5)$$

Another well-known isotherm is Freundlich isotherm. This linearized isotherm can be expressed by the following equation. Where K_F and n are the Freundlich isotherm constants related to adsorption capacity (mg/g) and intensity of adsorption, respectively.

$$\ln q_e = \ln K_F + \frac{1}{n}\ln C_e \quad (6)$$

Characterization: The chemical and physical features of the synthesized Cd-H_4bta were examined by SEM, TGA, XRD, FTIR and nitrogen adsorption-desorption. Scanning electron microscopy images were taken on a Nova Nano SEM 200 from FEI operated at 10.0 kV. Analytical Solutions Microtrac Nano-flex 180 DLS size was used to determine particle size distribution. For thermogravimetric analysis, a Perkin Elmer TGA 4000 was used; analyses were performed from 30 to 900 °C at a heating rate of 10 °C/min under a nitrogen atmosphere. Perkin Elmer Fourier transformed infrared spectroscopy FT-IR/FT-NIR spectrometer, spectrum 400 was used to affirm the organic functional groups. The measuring range extended from 4000 to 520 cm^{-1}. X-ray diffractometer (XRD), Shimadzu XRD 7000 was used to identify crystalline phase of the sample, scan range was set from 5 to 50 (2θ, °), scan speed was set at 1θ °/min. Nitrogen adsorption-desorption analysis was performed at liquid nitrogen temperature using a MicromeriticsTrista II surface area and porosity analyzer. The sample was degassed overnight at 60 °C. After adsorption studies, atomic adsorption spectroscopy (AAS) Shimadzu ASC 7000

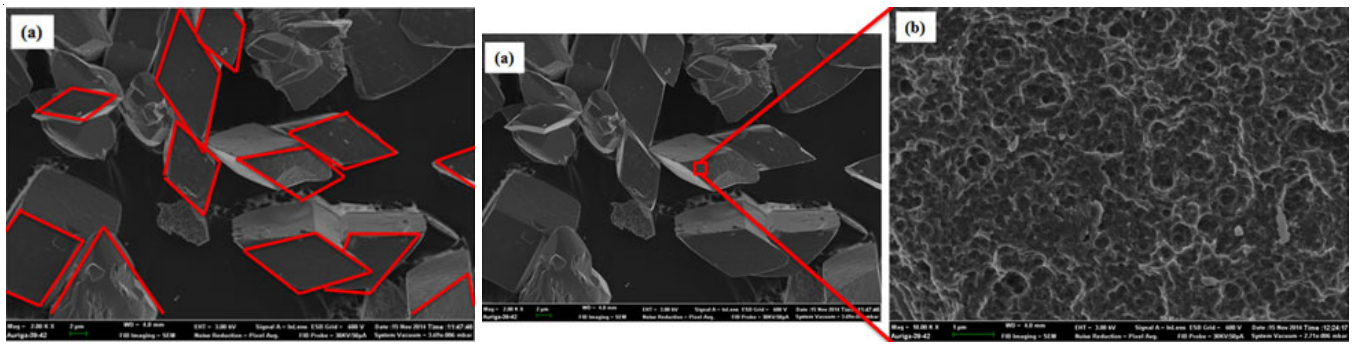

Fig. 1. SEM images of Cd-H_4bta; (a) rhombic prism crystals, (b) Cd-H_4bta surface

auto sampler was used to measure the remaining Pb(II), Cu(II) and Ni(II) ions in the sample solutions and traces of Cd(II) ions.

RESULTS AND DISCUSSION

Characterization of Cd-H_4bta MOFs: Fig. 1(a-d) presents synthesized Cd-H_4bta SEM images, particles size range distribution and BET surface properties. Fig. 1(a) is focalized on the over-view (general morphology of the particles) and Fig. 1(b) close-view of particles surface. As presented on Fig. 1(a), images of the general morphology of the synthesized material are predominantly constituted of rhombic prism crystals as indicated by red lines. Fig. 1(b) presents Cd-H_4bta surface. It was observed that these material exhibit crater like bumpy surface. On the magnification of the image presented in Fig. 1(b), it revealed spherical pores that are uniformly distributed on the particles surface. Particle size range distribution graph is presented in Fig. 1(c). It shows that over 80 % of the synthesized Cd-H_4bta particles ranged between 190-220 nm. This indicated the homogeneity of the size distribution.

Nitrogen adsorption-desorption test was conducted for further characterization of the porosity of Cd-H_4bta. Nitrogen adsorption-desorption isotherm is shown in Fig. 1(d). The results

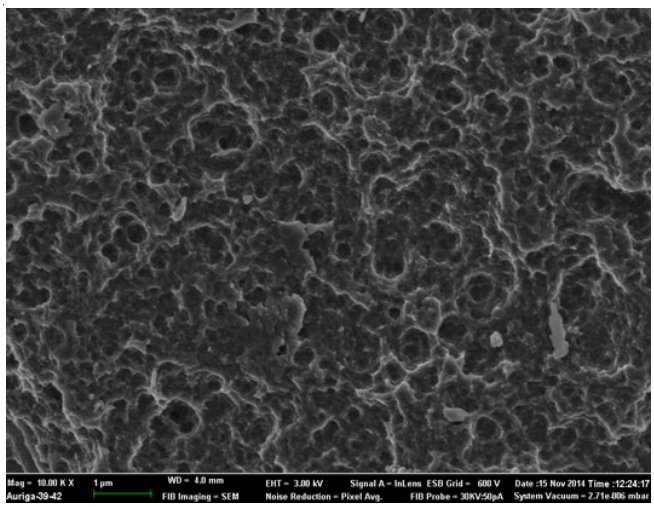

Fig. 1b. Cd-H_4bta porous surface

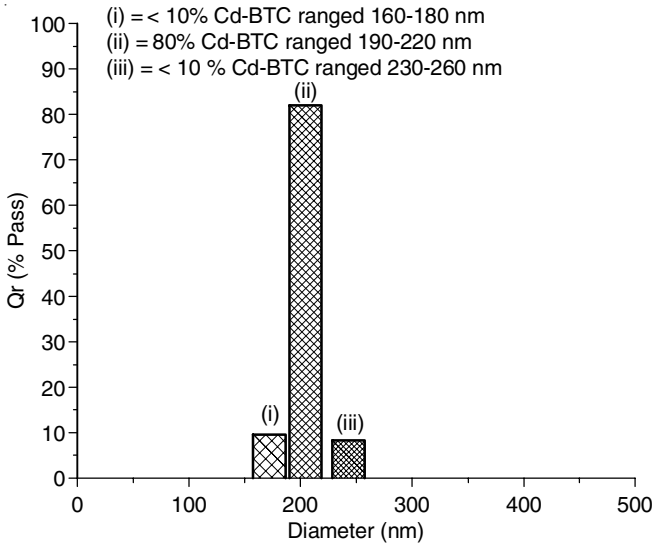

Fig. 1c. Cd-H_4bta size range distribution

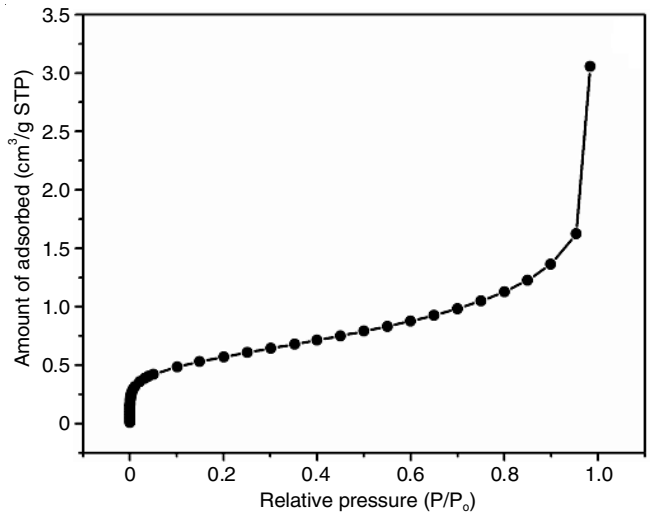

Fig. 1d. BET analysis, N_2 adsorption-desorption isotherm experiments at 77 K

determined specific surface area, pore volume (V_p) and pore diameter (d_p) is reported in Table-1. The obtained isotherm data revealed a typical Type IV adsorption. The profile pattern

TABLE-1
COMPARISON STUDY OF Cd-H_4bta MOFs, BET SURFACE PROPERTIES AGAINST OTHER CADMIUM COMPOSITES

Sample name	Morphology	BET surface area (m^2/g)	Pore diameter (d_p, nm)	Pore volume (V_p, cm^3/g)	Reference
Cd-H_4bta	Rhombic prism	0.714	0.1414	0.0194	This study

indicates that the material is microporous however it exhibited very low gas adsorption, even though the sample is highly porous. Suggesting only surface adsorption occurred. However the porosity aspect of the material is anticipated to enhance aqueous adsorption capability.

The XRD plot of Cd-H_4bta is presented in Fig. 2. The Cd-H_4bta composite exhibited multiple crystalline phases. Rhombohedral crystalline phase is indexed by the diffraction peaks at 2θ 23.46°, 32.42° and 39.90° (JCPDS card number 00-042-1342). Orthorhombic crystalline phase (JCPDS card number 00-033-1993) at 10.50° and 24.60° 2θ. Monoclinic crystalline phase (JCPDS card number 00-040-0760) at 16.23 and 20.40°. The XRD diffraction narrow peaks indicate that high quality crystalline Cd-H_4bta was synthesized.

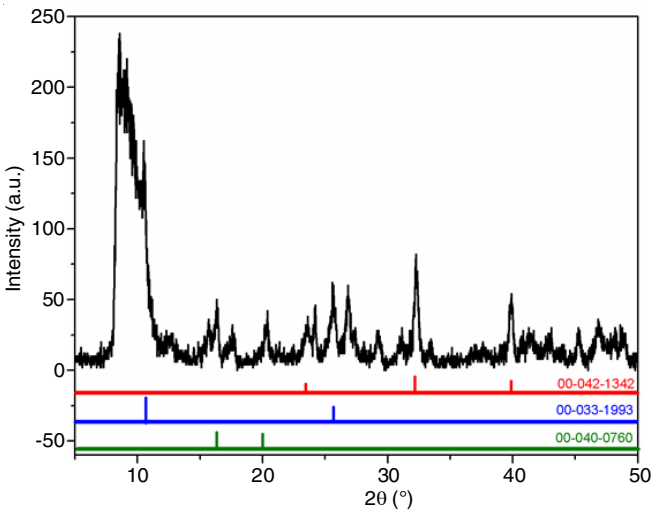

Fig. 2. XRD pattern of the as-synthesized Cd-H_4bta

Thermal stability of Cd-H_4bta MOFs was determined by thermogravimetry analysis (TGA) and differential thermal analysis (DTA) plots (Fig. 3). The TGA-DTA plots of Cd-H_4bta MOFs exhibited multiple breakdown steps. TGA plots confirmed a weight loss of 2.57 % also recorded by DTA plot at 49 °C this loss is consistent with the removal of unbound absorbed moister. TGA and DTA plots recorded two subsequent decompositions attributed to the loss of coordinated water (4.7 %) and DMF (3.32 %) molecules at 130 and 199 °C respectively. Then the anhydrous framework began to decompose, in two consecutive stages as confirmed by TGA and DTA plots. First the outer most bonds at 469 °C (lost weight: 30.36 %) and immediately followed by pyrolysis of inner bonds Cd-O at 515 °C (lost weight: 19.93 %). Thereafter, no further decomposition was observed and the remaining residue was recorded to be 25.70 %.

Fig. 4 presents the FTIR spectra of Cd-H_4bta. Stretching O–H vibrational frequency was observed at 3412 cm^{-1} due to COO^- and H_2O, bending frequency of O–H was seen at 1406 cm^{-1}. C=O and C-O were observed at 1616 and 1343 cm^{-1} respectively. The sp^2 bond C=C and C–C of the aromatic ring vibration frequencies were observed at 1663 and 1525 cm^{-1} respectively. C–H aromatic bonds were confirmed at a lower frequency, at 875 cm^{-1}. The vibration at 770 cm^{-1} is possibly due to Cd–O vibration, where the oxygen atom from benzene

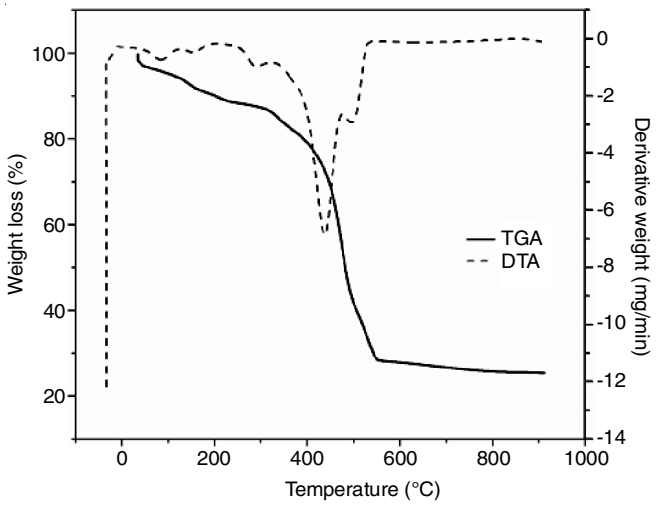

Fig. 3. TGA-DTA plots of the as-prepared Cd-H_4bta

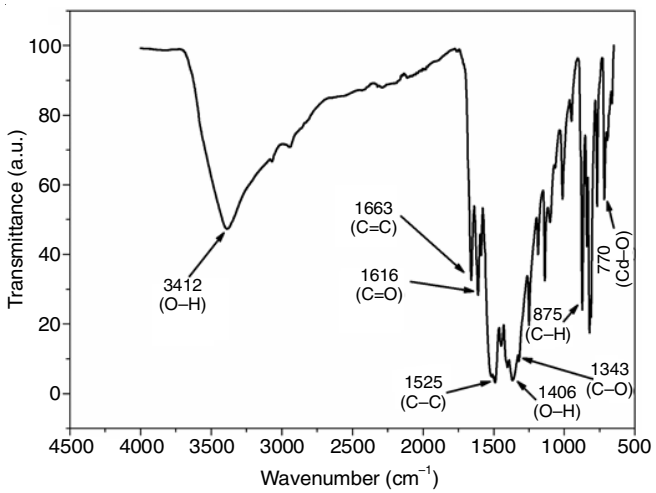

Fig. 4. FTIR spectra of Cd-H_4bta

1,2,4,5-tetracarboxylic acid is coordinated to the Cd. The FTIR spectra established the presence of carbonyl oxygen and hydroxyl functional groups. These groups are also anticipated to further enhance the adsorptive capability of the material.

The identified functional groups by FTIR spectra (Fig. 4) aided in predicting the structure of Cd-H_4bta. Fig. 5 presents a coordination environment of the Cd(II) ions in Cd-H_4bta; *i.e.* cadmium ion has coordination number (6). FTIR spectra confirmed that the skeletal of the as-prepared material is composed of oxygen containing functional groups and shown by the predicted structure (Fig. 5). These factors were essential for metal ions adsorption on Cd-H_4bta. These strongly influenced the adsorptive properties as illustrated in Fig. 6.

Adsorption of Cu(II), Pb(II) and Ni(II) ions on Cd-H_4bta

Effect of metal ions concentration on adsorption capacity (isotherms): Adsorption capacity is an important parameter, as it determines how much of Cd-H_4bta is required for quantitative enrichment of metal ions from a given solution. The adsorption capacity of Cd-H_4bta for Cu(II), Pb(II) and Ni(II) metal ions is demonstrated in Fig. 7. It was observed that the adsorption capacity of Cd-H_4bta increase with increasing metal ions concentration, this was due to the reinforcement of oxygen containing functional groups on the materials surface (FTIR

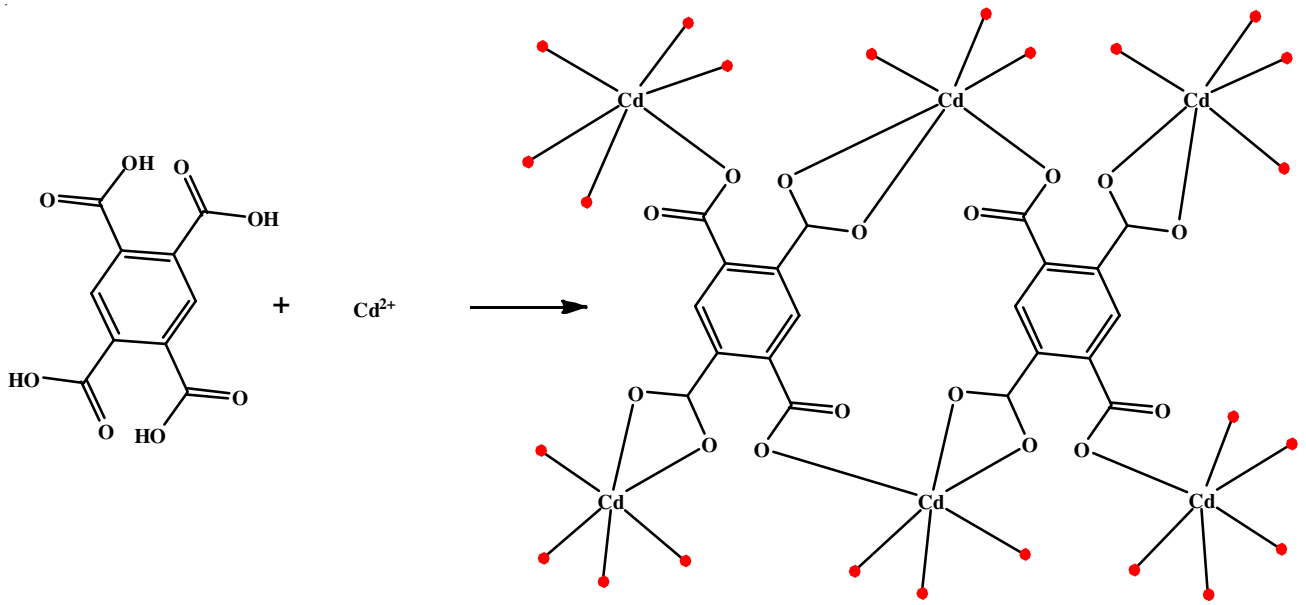

Fig. 5. Proposed coordination number of the Cd(II) ions with H_4bta is (6) to form Cd-H_4bta repeating units

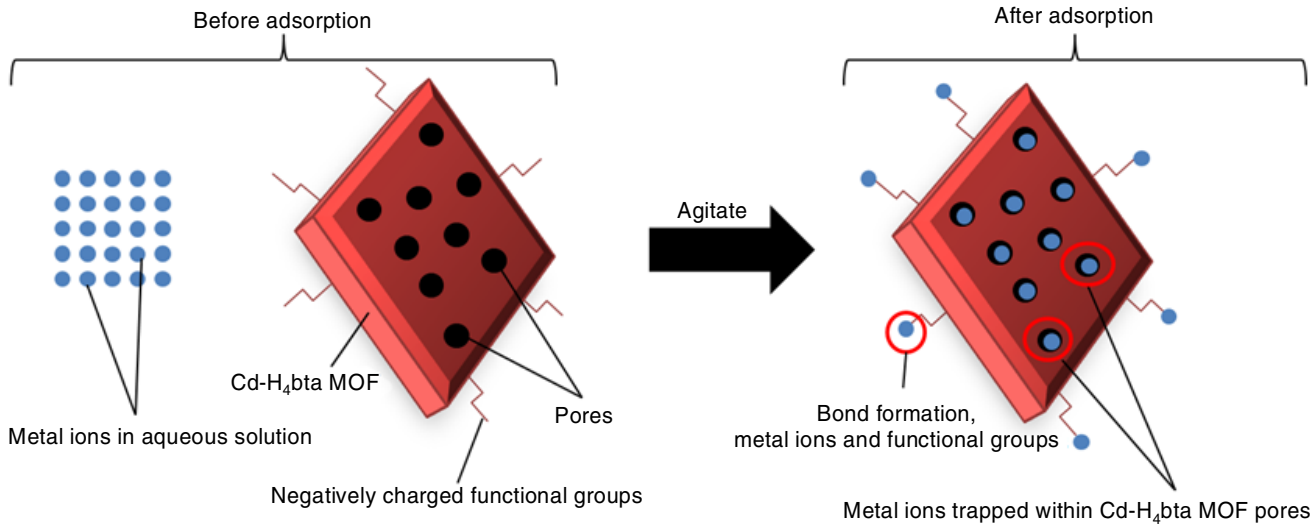

Fig. 6. Illustration diagram for the metal ions adsorption of Cd-H_4bta

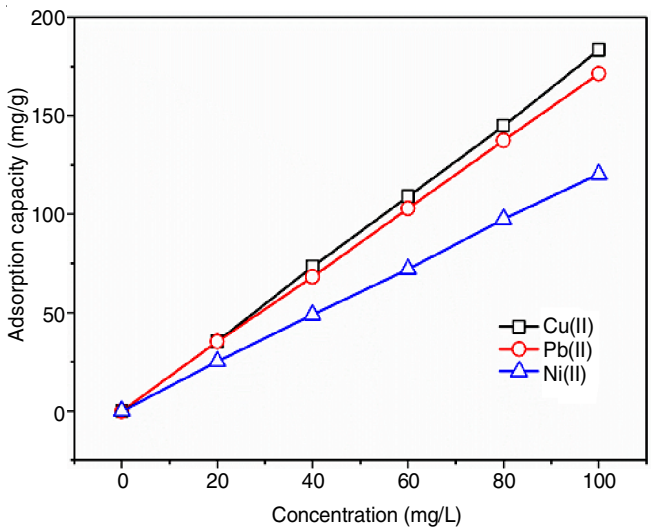

Fig. 7. Adsorption capacity of Cd-H_4bta towards metal ions (Cd-H_4bta: 0.1 g, metal ions solution volume: 0.02 L, 320 rmp, 25 °C, 30 min)

spectra) and its porous nature (SEM images) which in turn aid the surface area to enhance adsorption (Fig. 6) [29]. The adsorption capacities were as follows: 183.43 mg/g for Cu(II), 171.42 for Pb(II) and 120.31 for Ni(II) ions.

Effect of concentration on percentage removal: The effect of varying metal ions concentration (20, 40, 60, 80 and 100 mg/L) on the percentage removal of Cd-H_4bta was evaluated in triplicates for each concentration and other variables were fixed as presented on Fig. 8. The experimental data revealed that the percentage removal of Cu(II), Pb(II) and Ni(II) ions was higher in the 20 mg/L solutions. This was due to, more surface area and active sites were available and easily accessible. However higher metal ion solution concentrations experienced lower ions removal due to repulsion forces between metal ions, inhibited further adsorption; another factor may be exhausted surface area and active sites as they were being saturated [30]. The results presented are averages of experiments carried out in triplicates. These results show average of all triplicates.

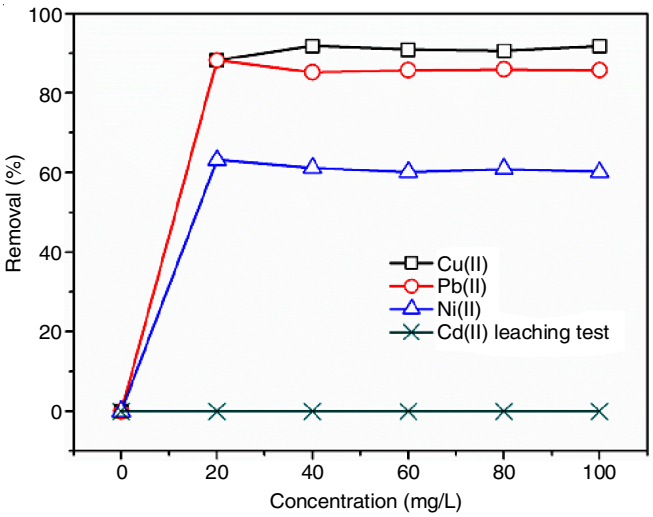

Fig. 8. Concentration effect of metal ions towards Cd-H_4bta, (Cd-H_4bta: 0.1 g, metal ion solution volume: 0.02 L, 320 rmp, 25 °C, 30 min)

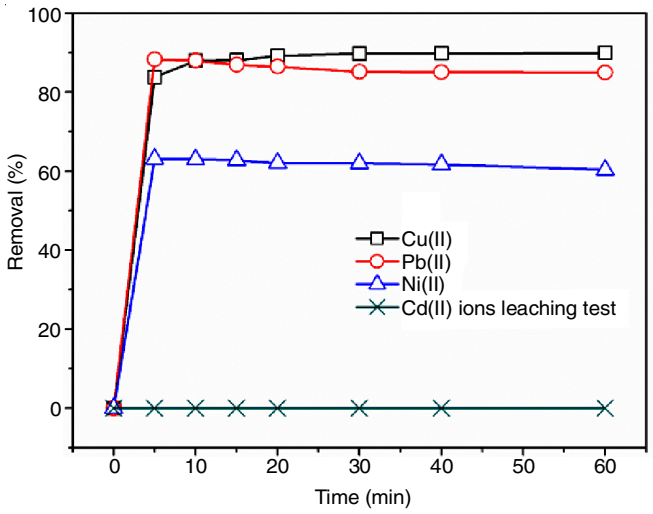

Fig. 9. Time effect of metal ions towards Cd-H_4bta, (Cd-H_4bta: 0.1 g, metal ion solution volume & concentration: 0.02 L & 100 mg/L, 320 rmp, 25 °C)

Effect of time on percentage removal: Influence of time was studied in triplicates at different intervals (5, 10, 15, 20, 30, 40 and 60 min) on the percentage removal of Cd-H_4bta and other variables were fixed as presented on Fig. 9. It was recorded that rapid adsorption occurred within the first 5 min, over 88 % for Cu(II), 83 % for Pb(II) and 63 % for Ni(II) ions were removed. However, it was also observed that metal ions reached equilibrium point at different time intervals, both Pb(II) and Ni(II) attained equilibrium from the 10 min mark and 20 min mark for Cu(II). At equilibrium, over 88 % for Pb(II), 63 % for Ni(II) and 89 % for Cu(II) was removed. Each plot shows average of results carried out in triplicates.

Kinetic studies: Adsorption experimental data of Pb(II), Cu(II) and Ni(II) were used to obtain kinetic parameters; pseudo first (PFO) and second order (PSO). Linear plots of PFO (In (q_e-q_t) *vs.* t) and PSO (t/q_t *vs.* t) were plotted to determine K_1 (equilibrium rate constant of pseudo first order kinetics), K_2 (equilibrium rate constant of pseudo second order kinetics) and R^2 are shown in Table-2. Best fitted correlation coefficient (R^2) values for Pb(II), Cu(II) and Ni(II) are those of (PSO) kinetic; R^2 = 0.9998, 0.9997 and 0.9999, respectively than those of PFO kinetic. This suggested that Cd-H_4bta followed a (PSO) kinetic mechanism. The sorption was controlled by valence interactions *via* sharing or exchanging of electrons and electrostatic forces between Cd-H_4bta and metal ions.

Isotherm studies: The applicability of Langmuir and Freundlich isotherms was investigated for Pb(II), Cu(II) and Ni(II) ions adsorption (Table-3). Best fitted isotherm mechanism is determined by the magnitude of correlation coefficient (R^2). The R^2 values for Freundlich isotherm mechanism were marginally greater. Langmuir-Freundlich (R^2) difference was 0.0033 for Pb(II), 0.0003 for Ni(II) and 0.0263 for Cu(II). This therefore could suggest that both isotherm mechanisms *i.e.*, Langmuir and Freundlich contributed in the metal adsorption process. However Freundlich isotherm better described the metals adsorption. Linearized Langmuir isotherm plotted graph of (C_e/q_e *vs.* C_e) gave values of Langmuir constant (K_L), Langmuir equilibrium constant (R_L) and correlation coefficient (R^2). Likewise, linear Freundlich isotherm plot of (ln C_e *vs.* ln q_e) was plotted, Freundlich constants (K_F) and (n) and (R^2). Langmuir and Freundlich constants (R_L) and (n) respectively were determined. Adsorption can either be; unfavourable when ($R_L > 1$), linear when ($R_L = 1$), favourable when ($0 < R_L < 1$), or irreversible when ($R_L = 0$). Obtained values of (R_L) indicated that sorption were favourable. Values for (n) show the type of isotherm; irreversible (n = 0), favourable ($0 < n < 1$), unfavourable ($n > 1$). Presented values of (n) show that Pb(II), Cu(II) and Ni(II) ions adsorption were favourable.

Cd-H_4bta stability test: Cadmium ions are among the most hazardous ones. During adsorption studies (concentration

TABLE-2
PSEUDO FIRST AND SECOND KINETIC ORDER FOR Pb(II), Cu(II) AND Ni(II) IONS SORPTION

Metal	q_{max} (mg/g)	Pseudo-first order (PFO)		Pseudo-second order (PSO)	
		K_1 (1/min)	R^2	K_2 (g/mg min)	R^2
Pb(II)	171.42	0.000288	0.9075	2.8236	0.9998
Cu(II)	183.43	0.000367	0.4964	3.0221	0.9997
Ni(II)	120.31	0.000290	0.9840	1.8467	0.9999

TABLE-3
ISOTHERM FOR Pb(II), Cu(II) AND Ni(II) IONS ADSORPTION

Metal	q_{max} (mg/g)	Langmuir isotherm			Freundlich isotherm		
		K_L (L/mg)	R_L	R^2	K_F ($mg^{1-n}L^n/g$)	N	R^2
Pb(II)	171.42	0.02700	0.6493	0.9863	0.2483	0.2811	0.9896
Cu(II)	183.43	0.02027	0.7115	0.9316	0.2132	0.1820	0.9579
Ni(II)	120.31	0.01917	0.7228	0.9983	0.4040	0.3750	0.9986

TABLE-4
ADSORPTION CAPACITY COMPARISON OF CADMIUM MOF WITH SOME METAL MOFs RELATIVE TO COPPER(II), LEAD(II) AND NICKEL(II) ADSORPTION

Cu(II)			Pb(II)			Ni(II)		
Adsorbent	Adsorption capacity (mg/g)	Ref.	Adsorbent	Adsorption capacity (mg/g)	Ref.	Adsorbent	Adsorption capacity (mg/g)	Ref.
MOF-NC	33.44	[31]	Co-MOF	85.72	[34]	Chitosan-MOF	60.0	[32]
Chitosan-MOF	50.6	[32]	Cu-MOF	71.36	[35]	Cd-MOF	120.31	This study
MOF, MIL-Fe	135.0	[33]	Fe-MOF	90.15	[36]			
Cd-MOF	183.43	This study	Zr-MOF	135.0	[37]			
			Cd-MOF	171.42	This study			

and time effect) subsequently Cd-H_4bta stability test was conducted (*i.e.* amount of cadmium ions that might have leached in to water samples). In Figs. 8 and 9 (-X-) marked plots were linear indicating that no cadmium ions were detected in the supernatant water samples. This confirms that the proposed Cd-H_4bta adsorbent is insoluble and does not leach cadmium ions and it is suitable and safe for aqueous solution use.

Comparative study: The adsorption capacities of Cu(II), Pb(II) and (Ni) ions are presented in Table-4. From these values, it is observed that Cd-H_4bta exhibited higher adsorption capacity than those reported for other MOFs. The maximum adsorption capacity value calculated for Cd-H_4bta was 183.43 mg/g in the removal of Cu(II) ions. This is a significant three-fold improvement over and above other recently reported MOF adsorbents such as MOF-MIL-Fe, MOF-NC and chitosan-MOF considered good adsorbents for Cu(II) ion adsorption [31-33]. MOF-MIL-Fe with an adsorption capacity of (135.0 mg/g) possess a lower (q_e) compared to Cd-H_4bta. The maximum calculated (q_e) value for Pb(II) ions was 171.42 mg/g. Co-MOF [34] have a maximum adsorption capacity corresponding to 50 % of the adsorption capacity value obtained for Cd-H_4bta while Cu-MOF [35], Fe-MOF [36] and Zr-MOF [37,38] have adsorption capacity corresponding to only 42, 53 and 79 % respectively. The maximum adsorption capacity values of Cd-MOF for Cu(II), Pb(II) and Ni(II) ion (183.43, 171.42 and 120.31 mg/g) respectively indicated that this material is a potential candidate for removing metal ions from aqueous solution.

Conclusion

In this research work, we have synthesized Cd-H_4bta and applied it as a potential adsorbent for the removal of Cu(II), Pb(II) and Ni(II) ions from solution. The synthesized material was confirmed by SEM, TGA, FTIR, XRD and BET. SEM and FTIR. The results showed that the synthesized material had high content of oxygen containing functional groups and pores on its surface. Therefore, the adsorption experimental data of the material in turn had the advantages of rapid adsorptive rate and higher sorption capacity. Cd-H_4bta adsorption capacities for Cu(II), Pb(II) and Ni(II); were 183.43, 171.42 and 120.31 mg/g respectively for solutions containing 100 mg/L ions of each metal. Kinetics data of Pb(II), Cu(II) and Ni(II), followed (PSO) kinetic model, their (R^2) correlation coefficient values were 0.9998, 0.9997 and 0.9999 respectively. This suggested that the adsorptive processes were of a chemical nature. The physical and chemical features of Cd-H_4bta; porosity and functional groups, were essential in metal ions removal from water. This paper suggests an ample adsorbent, that has high adsorption capacity for Cu(II), Pb(II) and Ni(II) ions in aqueous solution. It is concluded that Cd-H_4bta is a potential material.

ACKNOWLEDGEMENTS

This work was supported by research grant from the research directorate of the Vaal University of technology, Vanderbijlpark, South Africa.

REFERENCES

1. A.T. Jan, M. Azam, K. Siddiqui, A. Ali, I. Choi and Q.M.R. Haq, *Int. J. Mol. Sci.*, **16**, 29592 (2015); https://doi.org/10.3390/ijms161226183.
2. M. Jaishankar, T. Tseten, N. Anbalagan, K.N. Beeregowda and B.B. Mathew, *Interdiscip. Toxicol.*, **7**, 60 (2014); https://doi.org/10.2478/intox-2014-0009.
3. D.P. Sountharajah, P. Loganathan, J. Kandasamy and S. Vigneswaran, *Chemosphere*, **168**, 467 (2017); https://doi.org/10.1016/j.chemosphere.2016.11.045.
4. R. Nagarajah, K.T. Wong, G. Lee, K.H. Chu, Y. Yoon, N.C. Kim and M. Jang, *Sep. Purif. Technol.*, **174**, 290 (2017); https://doi.org/10.1016/j.seppur.2016.11.008.
5. P.B. Tchounwou, G.C.Yedjou, A.K. Patlolla and D.J. Sutton, *Mol. Clin. Environ. Toxicol.*, **101**, 133 (2014); https://doi.org/10.1007/978-3-7643-8340-4_6.
6. R. Singh, N. Gautam, A. Mishra and R. Gupta, *Indian J. Pharmacol.*, **43**, 246 (2011); https://doi.org/10.4103/0253-7613.81505.
7. G. Pandey and S. Madhuri, *Res. J. Anim. Veter. Fish. Sci.*, **2**, 17 (2014).
8. J.N. Gordon, A. Taylor and P.N. Bennett, *Br. J. Clin. Pharmacol.*, **53**, 451 (2002); https://doi.org/10.1046/j.1365-2125.2002.01580.x.
9. K.A. Adamama-Moraitou, T. Rallis, A. Papasteriadis, N. Roubies and N. Kaldrimidou, *Dig. Dis. Sci.*, **46**, 1444 (2001); https://doi.org/10.1023/A:1010635820071.
10. K.K. Das, S.N. Das and S.A. Dhundasi, *Indian J. Med. Res.*, **128**, 412 (2008).
11. S.S. Kalaivani, A. Muthukrishnaraj, S. Sivanesan and L. Ravikumar, *Process Saf. Environ. Prot.*, **104**, 11 (2016); https://doi.org/10.1016/j.psep.2016.08.010.
12. J. Wang, M. Xie, H. Wang and S. Xu, *Hydrometallurgy*, **167**, 39 (2017); https://doi.org/10.1016/j.hydromet.2016.10.020.
13. J.C. Yoo, C. Lee, J.-S. Lee and K. Baek, *J. Environ. Manage.*, **186**, 314 (2017); https://doi.org/10.1016/j.jenvman.2016.03.016.
14. C.G. Lee, P.J.J. Alvarez, A. Nam, S.J. Park, T. Do, U.-S. Choi and S.-H. Lee, *J. Hazard. Mater.*, **325**, 223 (2017); https://doi.org/10.1016/j.jhazmat.2016.12.003.
15. A. Graillot, C. Cojocariu, D. Bouyer, S. Monge, S. Mauchauffe, J.-J. Robin and C. Faur, *Sep. Purif. Technol.*, **141**, 17 (2015); https://doi.org/10.1016/j.seppur.2014.11.023.
16. L.X. Zhong, X.W. Peng, D. Yang and R. Sun, *J. Agric. Food Chem.*, **60**, 5621 (2012); https://doi.org/10.1021/jf301182x.

17. L. Appels, L. Baeyens, J. Degreve and R. Dewil, *Pror. Energy Combust. Sci.*, **34**, 755 (2008); https://doi.org/10.1016/j.pecs.2008.06.002.
18. S.N.A. Abas, M.H.S. Ismail, M.L. Kamal and S. Izhar, *World Appl. Sci. J.*, **28**, 1518 (2013); https://doi.org/10.5829/idosi.wasj.2013.28.11.1874.
19. M.R. Ryder and J.-C. Tan, *Mater. Sci. Technol.*, **30**, 1598 (2014); https://doi.org/10.1179/1743284714Y.0000000550.
20. L. Zeng, X. Guo, C. He and C. Duan, *ACS Catal.*, **6**, 7935 (2016); https://doi.org/10.1021/acscatal.6b02228.
21. Z. Saedi, V. Safarifard and A. Morsali, *Micropor. Mesopor. Mater.*, **229**, 51 (2016); https://doi.org/10.1016/j.micromeso.2016.04.017.
22. H.W.B. Teo, A. Chakraborty and S. Kayal, *Appl. Therm. Eng.*, **110**, 891 (2017); https://doi.org/10.1016/j.applthermaleng.2016.08.126.
23. S. Castarlenas, C. Téllez and J. Coronas, *J. Membr. Sci.*, **526**, 205 (2017); https://doi.org/10.1016/j.memsci.2016.12.041.
24. M.S. Hosseini, S. Zeinali and M.H. Sheikhi, *Sens. Actuators B Chem.*, **230**, 9 (2016); https://doi.org/10.1016/j.snb.2016.02.008.
25. S. Naeimi and H. Faghihian, *Sep. Purif. Technol.*, **175**, 255 (2017); https://doi.org/10.1016/j.seppur.2016.11.028.
26. H. Furukawa, K.E. Cordova, M. O'Keeffe and O.M. Yaghi, *Science*, **341**, 1230444 (2016); https://doi.org/10.1126/science.1230444.
27. T.T. Zheng, J. Zhao, Z.W. Fang, M.T. Li, C.-Y. Sun, X. Li, X.-L. Wang and Z.-M. Su, *Dalton Trans.*, **46**, 2456 (2017); https://doi.org/10.1039/C6DT04630D.
28. M. Yilmaz, T. Tay, M. Kivanc and H. Turk, *Braz. J. Chem. Eng.*, **27**, 309 (2010); https://doi.org/10.1590/S0104-66322010000200009.
29. A. Sankhla, R. Sharma, R.S. Yadav, D. Kashyap, S.L. Kothari and S. Kachhwaha, *Mater. Chem. Phys.*, **170**, 44 (2016); https://doi.org/10.1016/j.matchemphys.2015.12.017.
30. A.V. Borhade and B.K. Uphade, *Desalination Water Treat.*, **57**, 9776 (2016); https://doi.org/10.1080/19443994.2015.1041051.
31. M. Zhou, J. Li, Z. Ye, C. Ma, H. Wang, P. Huo, W. Shi and Y. Yan, *ACS Appl. Mater. Interfaces*, **7**, 28231 (2015); https://doi.org/10.1021/acsami.5b06997.
32. C.V. Reddy, N. Bandaru, J. Shim and S.V.P. Vattikuti, *Appl. Phys*., *A Mater. Sci. Process.*, **123**, 396 (2017); https://doi.org/10.1007/s00339-017-1013-3.
33. K. Bhattacharya, D. Parasar, B. Mondal and P. Deb, *Sci. Rep.*, **5**, 17072 (2015); https://doi.org/10.1038/srep17072.
34. N.D. Shooto, N. Ayawei, D. Wankasi, L. Sikhwivhilu and E.D. Dikio, *Asian J. Chem.*, **28**, 277 (2016); https://doi.org/10.14233/ajchem.2016.19202.
35. N.D. Shooto, E.D. Dikio, D. Wankasi and L. Sikhwivhilu, *Chem. Sci. J.*, **6**, 4 (2015).
36. N.D. Shooto, E.D. Dikio, D. Wankasi and L. Sikhwivhilu, *Hem. Ind.*, **71**, 221 (2017); https://doi.org/10.2298/HEMIND160120032S.
37. N. Yin, K. Wang and Z. Li, *Chem. Lett.*, **45**, 625 (2016); https://doi.org/10.1246/cl.160148.